BRAIN COMMUNICATIONS

Altered microstructure of the contralesional ventral premotor cortex and motor output after stroke

Paweł P. Wróbel,[1] Stephanie Guder,[1] Jan F. Feldheim,[1] José A. Graterol Pérez,[1] Benedikt M. Frey,[1] Chi-un Choe,[1] Marlene Bönstrup,[1,2] Bastian Cheng,[1] Yogesh Rathi,[3,4] Ofer Pasternak,[3,4] Götz Thomalla,[1] Christian Gerloff,[1] Martha E. Shenton[3,4] and Robert Schulz[1]

Cortical thickness analyses have provided valuable insights into changes in cortical brain structure after stroke and their association with recovery. Across studies though, relationships between cortical structure and function show inconsistent results. Recent developments in diffusion-weighted imaging of the cortex have paved the way to uncover hidden aspects of stroke-related alterations in cortical microstructure, going beyond cortical thickness as a surrogate for cortical macrostructure. We re-analysed clinical and imaging data of 42 well-recovered chronic stroke patients from 2 independent cohorts (mean age 64 years, 4 left-handed, 71% male, 16 right-sided strokes) and 33 healthy controls of similar age and gender. Cortical fractional anisotropy and cortical thickness values were obtained for six key sensorimotor areas of the contralesional hemisphere. The regions included the primary motor cortex, dorsal and ventral premotor cortex, supplementary and pre-supplementary motor areas, and primary somatosensory cortex. Linear models were estimated for group comparisons between patients and controls and for correlations between cortical fractional anisotropy and cortical thickness and clinical scores. Compared with controls, stroke patients exhibited a reduction in fractional anisotropy in the contralesional ventral premotor cortex ($P = 0.005$). Fractional anisotropy of the other regions and cortical thickness did not show a comparable group difference. Higher fractional anisotropy of the ventral premotor cortex, but not cortical thickness, was positively associated with residual grip force in the stroke patients. These data provide novel evidence that the contralesional ventral premotor cortex might constitute a key sensorimotor area particularly susceptible to stroke-related alterations in cortical microstructure as measured by diffusion MRI and they suggest a link between these changes and residual motor output after stroke.

1 Department of Neurology, University Medical Center Hamburg-Eppendorf, Hamburg 20251, Germany
2 Department of Neurology, University Medical Center, Leipzig 04103, Germany
3 Psychiatry Neuroimaging Laboratory, Brigham and Women's Hospital, Harvard Medical School, Boston 02115, MA, USA
4 Department of Radiology, Brigham and Women's Hospital, Harvard Medical School, Boston 02115, MA , USA

Correspondence to: Robert Schulz, MD
University Medical Center Hamburg-Eppendorf
Martinistraße 52, 20246 Hamburg, Germany
E-mail: rschulz@uke.de

Keywords: DWI; cortical; plasticity; unaffected; hemisphere

Abbreviations: ANTs = advance normalization tools; CC = corpus callosum; CT = cortical thickness; DWI = diffusion-weighted imaging; FA = fractional anisotropy; FW = free water; HMAT = human motor atlas template; M1 = primary motor cortex; NHP = nine-hole-peg test; NIHSS = National Institute of Health Stroke Scale; PMD = dorsal premotor cortex; PMV = ventral premotor cortex; preSMA = pre-supplementary motor area; SMA = supplementary motor area; S1 = primary somatosensory cortex; UEFM = upper extremity Fugl-Mayer

Received August 18, 2022. Revised March 17, 2023. Accepted May 15, 2023. Advance access publication May 17, 2023

Graphical Abstract

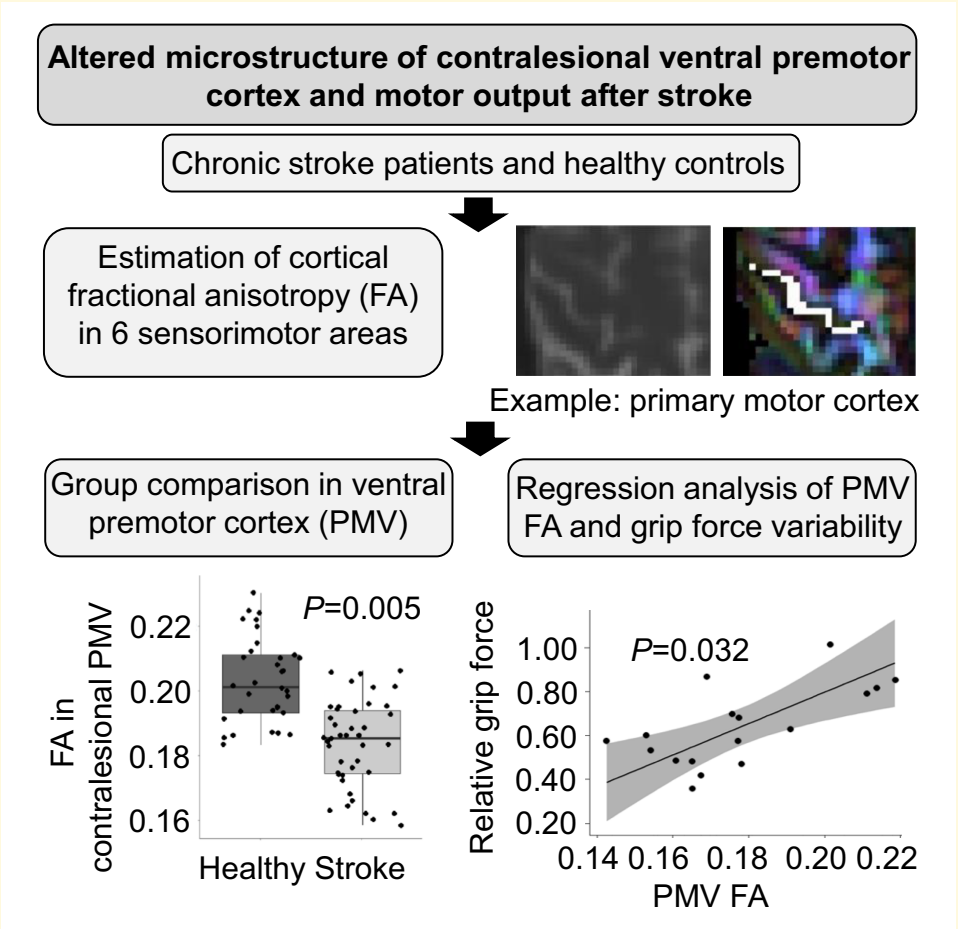

Introduction

The assessment of macrostructural cortical changes after ischaemic stroke by means of volumetric or surface-based cortical thickness (CT) analyses has significantly enhanced our current understanding of how acute stroke lesions lead to widespread changes in brain structure and how these may influence recovery processes.[1] Most studies have reported stroke-related cortical thinning in primary and secondary motor- and non-motor areas not only of the ipsilesional but also of the contralesional hemisphere.[2-9] Some studies have also shown increases in CT or grey-matter volume and argued that such findings might parallel neuroplastic brain changes, potentially promoting recovery after stroke.[10-13] However, studies exhibit a large variability in such results for group comparisons and particularly for correlational analyses between CT and residual function as well.[1] Recent developments have focused on layer-specific CT changes and their associations with clinical scores,[14] which suggests that, in addition to CT as a surrogate for macrostructure, measures of cortical microstructure might carry important information of stroke-related changes in brain structure with the potential to improve our current recovery models.

Over the last 25 years, diffusion-weighted imaging (DWI) has provided invaluable insights into changes in brain networks and microstructure after stroke.[15] Diffusion properties such as fractional anisotropy (FA), among others, have evolved as surrogate parameters for white-matter integrity. Technical limitations, such as free water (FW) contamination of DWI signals due to partial volume effects, have largely limited the application of DWI to cerebral white matter or deep subcortical grey matter.[16-20] Recently developed methods such as FW correction[21] or multi-shell DWI[16] have extended the possibilities for cortical DWI. The cortex is not only organized in different layers but also consists of capillaries, a variety of glia cells and neurons, which, in turn, display an intricate shape with the soma, axons, dendrites and synapses.[22] Diffusion tensor imaging (DTI) has demonstrated that the main diffusion direction, i.e. the orientation of the diffusion tensor, was oriented perpendicularly to the pial surface and highly corresponded with tensor information derived from brain histology.[23] Neuronal cell bodies, as well as the axons and apical dendrites of the neurons, were found to primarily contribute to this orientation. Together with other structures aligned orthogonally to the neurons, and parallel to the pial surface, these were also

reported to modulate anisotropy of the cortex. Dendritic arborization has been inversely correlated with the amount of anisotropy.[24,25] Dendrogenesis and synaptogenesis have been shown to reduce cortical FA over time during maturation.[26,27] In addition to FA, measures of regional variability of diffusion properties in the cortex have been related to clinical scores during aging processes.[28] These findings illustrate that cortical DWI might serve as an innovative tool to uncover yet hidden aspects of cortical microstructural changes and their relevance for recovery after stroke.

The aim of this retrospective study was to explore cortical diffusion properties in a large number of well-recovered chronic stroke patients. We re-analysed clinical and imaging data of patients with first-ever ischaemic stroke in the chronic stage of recovery, taken from two independent studies.[29-31] Following a region-of-interest approach, cortical FA was calculated for six key sensorimotor brain regions obtained from the human motor atlas template (HMAT).[32] CT was also estimated for these brain regions in order to compare microstructural findings with cortical macrostructure. The analyses were restricted to the contralesional hemisphere to exclude any direct lesion effects. Linear regression models were fit (i) to conduct group comparisons for cortical FA and CT between stroke patients and controls and (ii) to relate these measures to clinical scores of residual motor output.

Materials and methods

Participants and clinical data

Imaging and clinical data from chronic stroke patients and data from healthy controls of similar age and gender were re-analysed from two independent cohorts. Details of inclusion and exclusion criteria are given in the original reports.[29,33] In brief, patients had experienced a first-ever unilateral ischaemic stroke at least 6 months ago. A motor deficit of the upper limb was present, or it had been documented in the acute stage after stroke with subsequent improvement. Patients were at least 18 years old. Serious neurological or psychiatric comorbidities, contraindications against MRI or evidence for a recurrent stroke were exclusion criteria. All participants gave informed written consent, compliant with the Declaration of Helsinki. The studies were approved by the ethics committee at the Physicians' Chamber in Hamburg (PV3777 and PV5357). Figure 1 gives an overview of participant inclusion. Mean age of the stroke patients was 64 years, 71% were males and 38 were right-handed. Clinical testing included the National Institutes of Health Stroke Scale (NIHSS), the upper extremity Fugl-Meyer assessment (UEFM), grip strength (in kg, given as absolute and relative values: more affected/unaffected hand) and performance in the nine-hole-peg test (NHP, given as absolute values in pegs/s and as relative values). For group comparison, 42 patients and 33 healthy participants were analysed. Analyses for structure–outcome correlations were conducted primarily in a subset of patients with persistent motor deficits, operationalized by UEFM < 66. The rational for this approach was that previous studies have found that patients with complete or almost complete recovery were found to exhibit much weaker relationships between brain structure and outcome[34,35] and that structure–outcome relationships might be particularly driven by more impaired patients and might not generalize to patients with minor deficits.[36] Table 1 summarizes the demographic and clinical data.

Brain imaging: data acquisition, pre-processing and FW correction

Brain imaging was performed on a 3 T Siemens Skyra Scanner (Siemens Medical Solutions, Erlangen, Germany) with a 32-channel head coil. T_1-weighted imaging was based on a magnetization-prepared, rapid acquisition gradient-echo sequence (repetition time = 2.500 ms, echo time = 2.12 ms, 256 slices with a field of view = 240 × 192 mm and voxel size of 0.94 × 0.94 × 0.94 mm). DWI data sets consisted of 75 slices with 64 non-collinear gradient directions with a b-value of 1500 s/mm^2 as well as one b_0 image (echo time of 82 ms, repetition time 10 000 ms and voxel size of 2 × 2 × 2 mm). Pre-processing of DWI data sets included eddy current correction using the FSL (6.0.1)-based dwifslpreproc tool from MRtrix3 software (3.0.2) and correcting for phase encoding distortion by applying data from registration of the b_0 to the T_1 image using the antsRegistration tool from the advanced normalization tools (ANTs) package.[37-39] A custom-written MATLAB script (ran on Version R2020a; The Mathworks, Natick, MA, USA) was used to perform FW correction following the approach of Pasternak *et al.*[21] In brief, a bi-tensor model is calculated to predict the signal attenuation in the presence of FW contamination. The model includes two different compartments: The first compartment estimates the fractional volume of FW, which is modelled as an isotropic tensor with a fixed diffusivity. The other compartment uses a diffusion tensor to model water molecule diffusion in the vicinity of tissue membranes, from which eigenvalue maps corrected for FW are calculated. T_1-weighted images were processed using an ANT-based brain extraction tool as well as the *recon-all* tool from the FreeSurfer software (version 6.0.1).[40]

Brain imaging: diffusion properties of key sensorimotor areas and CT

The HMAT was used to identify six cortical key areas of the human sensorimotor network of the contralesional hemisphere, that are the primary motor cortex (M1), the primary somatosensory cortex (S1), the ventral and dorsal premotor cortex (PMV, PMD) as well as the pre-supplementary (preSMA) and the supplementary motor area (SMA).[32] HMAT atlas labels in Montreal Neurological Institute space were transformed non-linearly to the individual DWI space using the *flirt* and *fnirt* tools from FSL. The delineation of the final cortical labels was performed by the multiplication of each label with a binary cortex mask derived from the

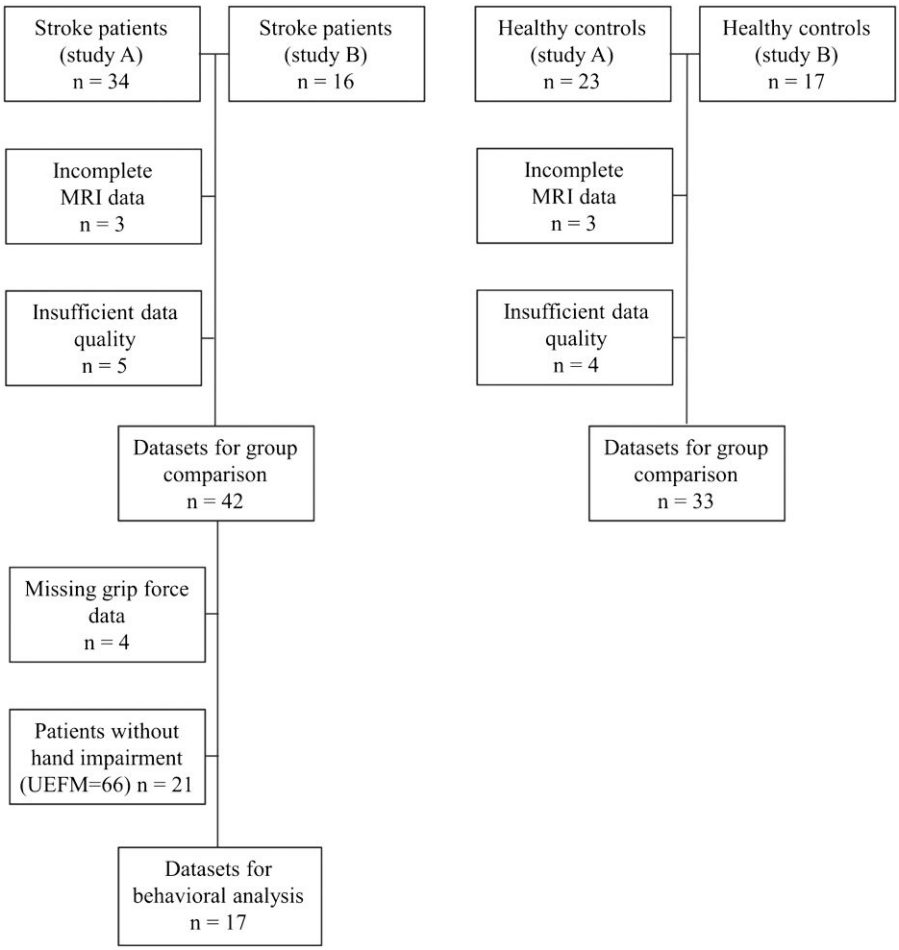

Figure 1 Flow chart of participant inclusions and exclusions. UEFM, upper extremity Fugl-Meyer.

FreeSurfer-generated *wmparc* file by merging all cortical labels into a cortex mask using *fslmaths*. HMAT labels were then multiplied with a binary mask of the label-specific lobe to avoid inclusion of voxels from other lobes. Regional mean CT of the six areas was estimated by registering the HMAT atlas data to the individual subject segmentation output using FreeSurfer's *vol2surf* and finally collected via *mri_segstats*. Mean values for cortical FA for each of the six areas were derived from the DTI volume consisting of the tensor eigenvalues using a custom-written MATLAB script (ran on Version R2020a; The Mathworks, Natick, MA, USA) as previously described.[28]

Statistical analysis

Statistics were performed using R software version 4.0.2. For group comparisons of cortical FA and CT, we estimated linear regression models with the cortical measures of interests as the dependent variable (DV) and GROUP (patients, controls) as the independent variable (IV) of interest. Separate models were calculated for all six regions of interest (ROIs), for cortical diffusion properties (six models) and CT values (six models). Target effects of the models were adjusted for the nuisance variables age, study, sex and lesion side (dominant or non-dominant hemisphere). In order to account for the distribution of affected hemispheres in the patients (dominant or non-dominant), the assignment of hemispheres in controls was pseudorandomized into pseudo-affected and a pseudo-unaffected hemisphere in line with previous studies.[41] In order to further explore the extent of Wallerian degeneration of inter-hemispheric transcallosal motor fibres originating in the ipsilesional hemisphere and projecting to contralesional sensorimotor areas as a potential influential factor for alterations in cortical FA, we estimated the FA of central segment of the corpus callosum (CC). This segment has been found to carry inter-hemispheric sensorimotor trajectories.[42-45] To this end, we used the FreeSurfer wmparc file already registered to the diffusion data. A linear model with cortical FA as DV and CC FA as IV was used and included age, affected hemisphere and study as nuisance variables. For structure–outcome inference, linear regression models were fit for relative grip force and NHP performance, NIHSS and UEFM as DV. These analyses were conducted in a subset of patients with persistent motor deficits as operationalized by UEFM < 66 ($n = 17$). Age, study and side of the lesion were included as nuisance variables to adjust the target effects. Statistical significance was assumed at $P < 0.05$.

Table 1 Demographic and clinical data of the patients

ID	Age	Gender	Dom	Side	Localization	NIHSS	UEFM	Grip force (kg) AH|UH		NHP (pegs/s) AH|UH		Grip force (rel.)	NHP (rel.)
01	56	Male	Left	Right	IC, BG	5	6						
02	69	Male	Left	Right	MCA-C	6	5						
03	62	Male	Left	Left	IC, BG	0	66	33.4	42.3	0.8	0.8	0.8	1.0
04	69	Male	Right	Right	MCA-C	0	66	47.7	53.3	0.6	0.8	0.9	0.8
05	68	Female	Left	Right	BS	0	66	23.2	21.8	0.8	0.9	1.1	0.9
06	71	Male	Left	Right	IC	0	66	37.3	37.7	0.6	0.7	1.0	0.8
07	65	Male	Left	Left	IC, BG	0	66	30.8	33.8	0.8	0.7	0.9	1.1
08	73	Female	Left	Right	MCA-C	0	66	25.7	28.5	0.6	0.9	0.9	0.7
09	58	Male	Left	Right	BS	2	58	23.7	45.0	0.7	0.9	0.5	0.7
10	73	Female	Left	Left	IC, BG	6	6	7.9					
11	56	Female	Left	Right	MCA-C	0	66	32.7	36.0	0.9	1.0	0.9	0.9
12	72	Female	Left	Left	BS	0	65	25.7	24.7	0.8	0.8	1.0	1.0
13	49	Male	Left	Left	MCA-C	0	66	49.3	48.3	1.0	1.1	1.0	1.0
14	63	Male	Left	Left	IC, BG	0	66	38.7	43.7	0.8	0.9	0.9	0.9
15	70	Female	Left	Right	MCA-C	1	65	19.0	26.0	0.6	0.8	0.7	0.7
16	65	Male	Right	Left	MCA-C	5	13		54.7		0.6		
17	85	Female	Left	Right	MCA-C	3	50	8.7	21.0		0.5	0.4	
18	81	Male	Left	Left	BS	0	66	41.0	40.0	0.5	0.5	1.0	1.0
19	44	Male	Right	Left	MCA-C	1	66	37.7	45.7	0.9	1.0	0.8	0.8
20	78	Female	Left	Left	IC, BG	0	66	26.3	24.0	0.9	0.9	1.1	1.0
21	47	Female	Left	Right	MCA-C	2	64	18.7	23.7	0.5	0.9	0.8	0.6
22	81	Male	Left	Left	MCA-C	3	63	24.7	28.0	0.4	0.5	0.9	0.8
23	76	Male	Left	Left	BS	0	66	42.0	41.0	0.6	0.7	1.0	0.9
24	55	Male	Left	Left	IC, BG	0	66	32.0	25.0	0.9	0.8	1.3	1.2
25	48	Male	Left	Left	A-/MCA-C	2	66	53.3	48.0	0.8	0.5	1.1	1.3
26	66	Male	Right	Right	MCA-C	2	66	54.6	52.7	0.6	0.9	1.0	0.7
27	47	Male	Left	Right	IC, BG	2	44	7.6	34.0		0.8	0.2	
28	77	Male	Left	Left	IC, BG	3	60	36.3	40.3	0.4	0.6	0.9	0.6
29	78	Female	Left	Left	IC, BG	0	66	19.3	24.0	0.8	0.8	0.8	1.0
30	74	Male	Left	Left	IC	0	66	42.0	34.7	0.6	0.5	1.2	1.0
31	73	Female	Left	Right	MCA-C	4	52	9.7	19.3	0.3	0.7	0.5	0.4
32	61	Male	Left	Right	MCA-C	0	66	28.7	45.3	0.7	0.7	0.6	0.9
33	55	Male	Left	Left	IC, BG	3	66	46.3	45.3	0.7	0.9	1.0	0.7
34	54	Male	Left	Left	IC	2	59	17.3	42.0	0.6	0.7	0.4	0.8
35	61	Male	Left	Left	IC, BG	3	47	31.0	42.7	0.5	0.9	0.7	0.6
36	76	Male	Left	Left	IC, BG	2	50	24.3	31.7	0.4	0.8	0.8	0.6
37	61	Male	Left	Left	PLIC	0	64	31.0	34.7	0.7	0.7	0.9	1.0
38	60	Male	Left	Left	IC, BG	2	55	35.3	43.3	0.6	0.8	0.8	0.8
39	58	Male	Left	Left	IC, BG	0	66	24.0	22.3	0.9	0.9	1.0	1.1
40	64	Male	Left	Right	IC, BG	4	52	4.3	21.3	0.5	0.8	0.2	0.6
41	63	Male	Left	Left	IC, BG	4	51	20.3	46.0	0.5	1.0	0.4	0.5
42	84	Female	Left	Left	IC, BG	2	39	9.3	15.0	0.4	0.7	0.6	0.6

Mean age in years: stroke group—63.86 (SD: 10.86), control group—66. (SD: 11.56), $P = 0.279$ (*t*-test) (median age: stroke group—65 years, healthy controls—69 years). Gender ratio (♂:♀) stroke group 71%:29%; control group 65%:35%, $P = 0.621$ (Fisher's exact test). Handedness ratio (r:l): stroke group—38:4, control group—41:1, $P = 0.315$ (Fisher's exact test). Median NIHSS in stroke patients: 1; median UEFM: 65; median relative grip force: 0.92; median NHP: 0.88. AH, affected hand; BG, basal ganglia; BS, brainstem; IC, internal capsule; Dom, dominant hemisphere; MCA-C, *arteria cerebri* media ischaemia with cortical and subcortical lesions; Rel, relative; Side, affected hemisphere; UH, unaffected hand.

Results are presented uncorrected (P) and corrected for multiple comparisons using the FDR method (P_{FDR}).[46] Robustness of the findings was further assessed by leave-one-out model analyses. Further details are given in the relevant sections.

Results

Cortical diffusion properties and thickness after stroke

Table 2 summarizes the results of the group comparison for regional FA and CT. We found a significant reduction in mean FA in the contralesional PMV ($P < 0.001$, $P_{FDR} = 0.005$). Relative average FA reduction was achieved 12% in patients, compared with controls. For CT of PMV, a numerical group difference with lower CT in patients (4% compared with controls) did not survive correction for multiple comparisons ($P = 0.035$, $P_{FDR} = 0.21$, Table 2, Fig. 2). The other regions did not show any significant group differences, neither in FA nor in CT. FA of the central segment of the CC was integrated with PMV FA to explore the influence of secondary Wallerian degeneration. We found a significant association [coefficient 0.300, 95% confidence interval (CI): 0.152–0.447, $P = 0.001$] with CC FA explaining 21% in PMV FA variability.

Table 2 Cortical diffusion properties and thickness after stroke

Variable	Controls (95% CI)	Stroke (95% CI)	*P*	P_{FDR}
FA M1	0.108 (0.099–0.117)	0.104 (0.096–0.113)	0.498	0.501
FA PMD	0.097 (0.097–0.111)	0.098 (0.092–0.105)	0.245	0.490
FA PMV	0.207 (0.196–0.218)	0.182 (0.171–0.193)	<0.001*	0.005*
FA preSMA	0.106 (0.097–0.116)	0.095 (0.086–0.105)	0.087	0.261
FA SMA	0.112 (0.101–0.122)	0.107 (0.097–0.117)	0.501	0.501
FA S1	0.119 (0.108–0.131)	0.112 (0.101–0.123)	0.333	0.499
CT M1	1.94 (1.89–2.00)	1.91 (1.86–1.96)	0.365	0.743
CT PMD	2.33 (2.26–2.40)	2.29 (2.22–2.35)	0.380	0.743
CT PMV	2.41 (2.35–2.48)	2.32 (2.26–2.39)	0.035	0.210
CT preSMA	2.67 (2.57–2.76)	2.63 (2.53–2.72)	0.522	0.743
CT SMA	2.47 (2.38–2.57)	2.45 (2.33–2.58)	0.759	0.759
CT S1	1.89 (1.84–1.93)	1.87 (1.83–1.92)	0.619	0.743

Estimated mean values (with 95% CI) are given for cortical FA and CT for stroke patients ($n = 42$) and controls ($n = 33$). Level of significance is given for the main effect GROUP without (*P*) and with correction for six comparisons for FA and CT each (P_{FDR}). * indicates a significant finding with *P*-value <0.05.

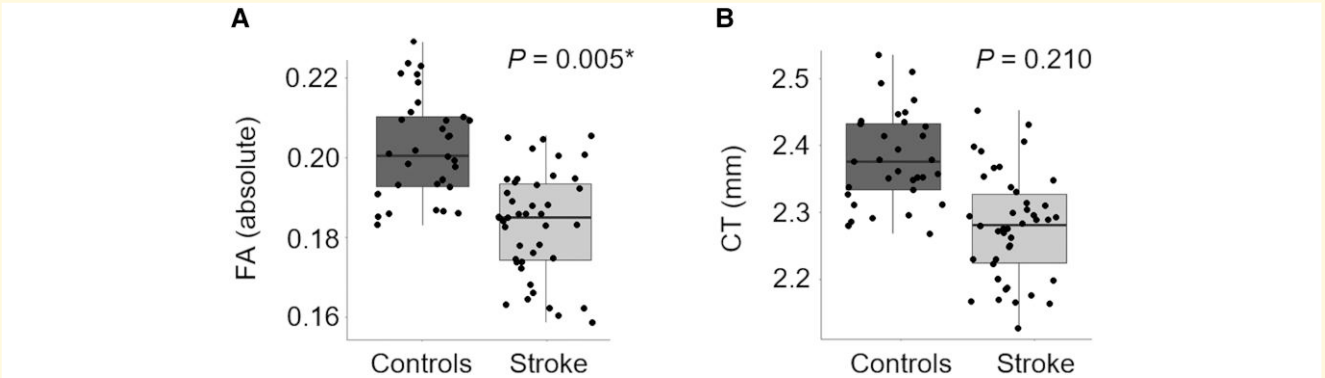

Figure 2 (A) FA and (B) CT of contralesional PMV in patients and controls. Estimated mean values from linear regression models of FA and CT for the contralesional PMV are illustrated by boxplots for stroke patients ($n = 42$) and controls ($n = 33$). While the group was the IV, additional nuisance variables included age, dominance of the affected hemisphere, study and gender. Dots indicate individual estimates.

Structure–outcome relationships

We explored structure–outcome relationships for FA/CT of contralesional PMV. We detected a linear positive association between FA of PMV and relative grip force ($P = 0.004$, $P_{FDR} = 0.032$). In the models, the inclusion of FA reduced the unexplained variance by 47%. In comparison, CT of PMV did not show any associations with grip force ($P = 0.302$, $P_{FDR} = 0.459$, Table 3, Fig. 3). For NHP, NIHSS and UEFM, neither FA nor CT of PMV did show any structure–outcome relationships.

Discussion

The main finding of the present work was that chronic stroke patients exhibit significant alterations in diffusion measures as surrogate parameters for the cortical microstructure of the contralesional PMV. These changes were related to residual grip force. CT as the more widely established marker was not able to capture these changes after stroke, nor was it associated with grip force. These data provide novel evidence that contralesional PMV might constitute a key motor area which seems to be specifically susceptible to stroke-related changes in cortical microstructural which may be directly linked with residual motor output.

Studies in animals and stroke patients have provided valuable insights into processes of functional and structural reorganization in contralesional premotor cortices which relate to recovery after stroke. For instance, studies in monkeys have reported increased contralesional PMV activation as measured by near-infrared spectroscopy[47] or by *c-fos* labelling for neuronal activity after stem cell treatment to promote recovery.[48] Regarding structural reorganization, other studies have highlighted lesion-size-dependent alterations of distal forelimb representations in ipsilesional PMV after M1 lesioning.[49,50] In stroke patients, a comparable upregulation of contralesional PMV activity, particularly in more impaired patients, has been reported across studies and meta-analyses.[51-53] Data for structural changes in contralesional brain areas underlying PMV is sparse. Some reports did not find any significant alterations,[4,8,11] others showed

Table 3 Structure–outcome relationships in stroke patients

Outcome	Variable	Coef.	95% CI Lower|upper	Adj. R^2	*P*	P_{FDR}
Grip force	FA PMV	7.43×10^3	3.67×10^3 to 11.18×10^3	0.501	0.004*	0.032*
	CT PMV	0.38	−0.25 to 1.02	0.073	0.302	0.483
NHP	FA PMV	-2.30×10^3	-8.81×10^3 to 4.20×10^3	0.407	0.536	0.536
	CT PMV	0.28	−0.44 to 1.01	0.411	0.501	0.536
NIHSS	FA PMV	4.19×10^3	-2.94×10^3 to 8.68×10^3	0.202	0.122	0.246
	CT PMV	−5.93	−12.28 to 0.42	0.202	0.123	0.246
UEFM	FA PMV	-319×10^3	-631×10^3 to -73.68×10^3	0.082	0.093	0.246
	CT PMV	23.20	−24.14 to 70.54	0.052	0.405	0.536

Influence of FA and CT of contralesional PMV on relative grip force, relative NHP performance, NIHSS and UEFM in stroke patients ($n = 17$). Coefficients (Coef.) are given with their 95% CIs. Level of significance is given for the main effect GROUP without (*P*) and with correction for eight tests (P_{FDR}). Explained variance of the complete model is given as adjusted R^2.
* indicates a significant finding with P-value<0.05.

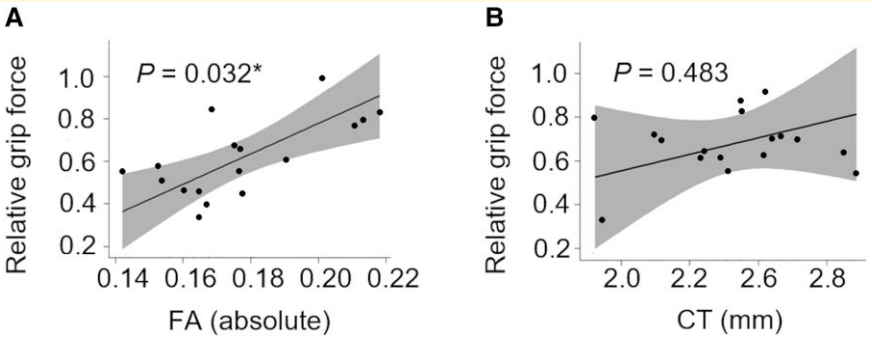

Figure 3 (A) Relationship between FA and (B) CT of contralesional PMV and relative grip force after stroke. Effect plots (including 95% CIs) are given for the linear regression models on relative grip force and FA and CT of contralesional PMV in stroke patients ($n = 17$), accounting for nuissance variables age, dominance status and study. Dots indicate individual estimates.

increases in CT.[10] Likewise, also the association between CT of ipsilesional and contralesional brain regions and motor functions is still under debate given positive[6,11,12,14] and negative[2,4,5,9,10] study results.

The present analyses provide novel insights into alterations of surrogate parameters for cortical microstructure in the contralesional PMV by showing significant reductions in FA in stroke patients. How can these findings be interpreted? Previous diffusion studies have reported that cortical anisotropy is influenced not only by principal neuronal cell bodies including axons and apical dendrites, but also by structures aligned orthogonally to the neurons, and parallel to the pial surface which contribute to dendritic arborization.[24,25] On one hand, this might be due to stroke-related dendrogenesis and synaptogenesis, which could lead to an increase in the amount of dendritic arborization. On the other hand, the decrease in cortical FA might also be the consequence of secondary Wallerian degeneration of principal neurons due to the stroke lesion as PMV neurons exhibit strong transcallosal inter-hemispheric connections.[54-56] Indeed, cortical degeneration in spared brain areas has already been linked to the extent of their connectivity to the stroke lesion.[4] It might follow secondary degeneration of principal neurons. Given consistent evidence of PMV upregulation in functional imaging, one could speculate that the FA reduction observed in the present cohort is likely to be the consequence of a combined process of Wallerian degeneration and compensational increasing arborization. However, as the amount of degeneration of transcallosal motor fibres, assessed by means of CC FA, only accounted for 21% of PMV FA variability, we would argue that mere Wallerian degenerative processes of PMV principal neurons are unlikely to explain our findings, but non-degenerative, potentially plastic cortical processes are likely to contribute as well. Such changes might parallel the contralesional brain's attempt to compensate for the motor deficits, an attempt that seems to be insufficient in the end. Discrepancies from previous reports showing increases in cortical FA in contralesional M1 and premotor areas might be due to the abdication of FW correction for FA estimation, differences in the time after stroke or the small sample size.[16]

We explored six key sensorimotor areas of the contralesional hemisphere. Absent changes in diffusion properties or significant structure–outcome relationships in these alternative areas, particularly in M1 or PMD, were intriguing. Like PMV, studies have shown that these motor areas of the contralesional hemisphere significantly contribute to residual motor functioning and recovery processes after stroke as well.[51,57,58] If true negative, this result would indicate that contralesional PMV was specifically susceptible to

microstructural changes which can be captured by cortical DWI. This view would be corroborated by reports showing that primary sensory/auditory/visual cortices show different maturation patterns compared with non-primary cortices[27] or that cortices differ in their microstructural characteristics such as the amount of neuropil.[59]

The diffusion parameter findings were contrasted with CT as an established macrostructural measure of cortical integrity which did not show comparably strong alterations in stroke patients, nor did CT exhibit any associations with residual motor output in the present cohort. Since neuronal degeneration and dendrogenesis and synaptogenesis occurs on the microscopic scale and the cortex consists of >50% of cells other than neurons,[22,59] the analysis of cortical diffusion might serve as a valuable novel tool with synergistic potential in addition to layer-specific thickness analyses[14] for stroke recovery research.

There are several limitations to note. First, across both groups, FA in PMV was higher when compared with other regions. This might be due to PMV-specific cortical architecture[59] with cortical FA values ranging between 0.1 and 0.3 in different cortices.[23] Alternatively, this finding might be explained by white-matter partial volume effects or differences in the size of the HMAT label masks. However, mean sizes for the masks were 437 voxels for PMV, but 374 voxels for M1 and 734 voxels for PMD. Hence, this factor is unlikely to cause any systematic error. Second, the cohort consisted of relatively well-recovered stroke patients with heterogeneous stroke locations in the chronic stage of recovery. To what extent the present findings will generalize to more severely impaired patients and more heterogeneous lesion topography remains a topic for upcoming studies. Third, the analyses were limited to the contralesional hemisphere in order to exclude direct lesion effects on the cortex. The existence of similar group differences and structure–outcome relationships for ipsilesional cortices cannot be excluded. Analyses in specific subgroups, e.g. patients with isolated subcortical strokes, would be needed to allow valid assessments of cortical microstructure of the ipsilesional hemisphere. Finally, aspects of the interpretation regarding the underlying pathophysiology and histology of our findings remain speculative. Prospective studies in independent cohorts are necessary to verify our results and translational longitudinal work is needed combining cortical DWI and histology in animal stroke models.

Funding

This work was supported by the Deutsche Forschungsgemeinschaft (DFG, German Research Foundation: 178316478, projects C1 to C.G., C2 to G.T.), the National Science Foundation of China (NSFC) and German Research Foundation (DFG; in project Crossmodal Learning, SFB TRR169/A3 to C.G.), the Werner Otto Stiftung (4/90 to R.S.). R.S. and C.C. are supported by an Else Kröner Exzellenzstipendium from the Else Kröner-Fresenius-Stiftung (2020_EKES.16 to R.S., 2018_EKES.04 to C.C.).

Competing interests

The authors report no competing interests.

Data availability

Data will be made available upon reasonable request.

References

1. Cortese AM, Cacciante L, Schuler AL, Turolla A, Pellegrino G. Cortical thickness of brain areas beyond stroke lesions and sensorymotor recovery: A systematic review. *Front Neurosci*. 2021;15:764671.
2. Buetefisch CM, Revill KP, Haut MW, *et al*. Abnormally reduced primary motor cortex output is related to impaired hand function in chronic stroke. *J Neurophysiol*. 2018;120(4):1680-1694.
3. Zhang J, Meng L, Qin W, Liu N, Shi F-D, Yu C. Structural damage and functional reorganization in ipsilesional M1 in well-recovered patients with subcortical stroke. *Stroke*. 2014;45:788-793.
4. Cheng B, Schulz R, Bonstrup M, *et al*. Structural plasticity of remote cortical brain regions is determined by connectivity to the primary lesion in subcortical stroke. *J Cereb Blood Flow Metab*. 2015;35(9):1507-1514.
5. Jones PW, Borich MR, Vavsour I, Mackay A, Boyd LA. Cortical thickness and metabolite concentration in chronic stroke and the relationship with motor function. *Restor Neurol Neurosci*. 2016;34(5):733-746.
6. Brodtmann A, Pardoe H, Li Q, Lichter R, Ostergaard L, Cumming T. Changes in regional brain volume three months after stroke. *J Neurol Sci*. 2012;322(1-2):122-128.
7. Hong H, Yu X, Zhang R, *et al*. Cortical degeneration detected by neurite orientation dispersion and density imaging in chronic lacunar infarcts. *Quant Imaging Med Surg*. 2021;11(5):2114-2124.
8. Chen H, Shi M, Geng W, Jiang L, Yin X, Chen Y-C. A preliminary study of cortical morphology changes in acute brainstem ischemic stroke patients. *Medicine (Baltimore)*. 2021;100(1):e24262.
9. Cheng B, Dietzmann P, Schulz R, *et al*. Cortical atrophy and transcallosal diaschisis following isolated subcortical stroke. *J Cereb Blood Flow Metab*. 2020;40(3):611-621.
10. Liu H, Peng X, Dahmani L, *et al*. Patterns of motor recovery and structural neuroplasticity after basal ganglia infarcts. *Neurology*. 2020;95(9):e1174-e1187.
11. Diao Q, Liu J, Wang C, *et al*. Gray matter volume changes in chronic subcortical stroke: A cross-sectional study. *Neuroimage Clin*. 2017;14:679-684.
12. Abela E, Seiler A, Missimer JH, *et al*. Grey matter volumetric changes related to recovery from hand paresis after cortical sensorimotor stroke. *Brain Struct Funct*. 2015;220(5):2533-2550.
13. Sterr A, Dean PJ, Vieira G, Conforto AB, Shen S, Sato JR. Cortical thickness changes in the non-lesioned hemisphere associated with non-paretic arm immobilization in modified CI therapy. *Neuroimage Clin*. 2013;2:797-803.
14. Lotan E, Tavor I, Barazany D, *et al*. Selective atrophy of the connected deepest cortical layers following small subcortical infarct. *Neurology*. 2019;92(6):e567-e575.
15. Koch P, Schulz R, Hummel FC. Structural connectivity analyses in motor recovery research after stroke. *Ann Clin Transl Neurol*. 2016;3(3):233-244.
16. Boscolo Galazzo I, Brusini L, Obertino S, Zucchelli M, Granziera C, Menegaz G. On the viability of diffusion MRI-based microstructural biomarkers in ischemic stroke. *Front Neurosci*. 2018;12:92.
17. Munoz Maniega S, Bastin ME, Armitage PA, *et al*. Temporal evolution of water diffusion parameters is different in grey and white

matter in human ischaemic stroke. *J Neurol Neurosurg Psychiatry*. 2004;75(12):1714-1718.
18. Molko N, Pappata S, Mangin JF, *et al*. Diffusion tensor imaging study of subcortical gray matter in cadasil. *Stroke*. 2001;32(9): 2049-2054.
19. Santos TEG, Baggio JAO, Rondinoni C, *et al*. Fractional anisotropy of thalamic nuclei is associated with verticality misperception after extra-thalamic stroke. *Front Neurol*. 2019;10:697.
20. Zhu LH, Zhang ZP, Wang FN, Cheng QH, Guo G. Diffusion kurtosis imaging of microstructural changes in brain tissue affected by acute ischemic stroke in different locations. *Neural Regen Res*. 2019;14(2):272-279.
21. Pasternak O, Sochen N, Gur Y, Intrator N, Assaf Y. Free water elimination and mapping from diffusion MRI. *Magn Reson Med*. 2009; 62(3):717-730.
22. Bourgeois JP, Rakic P. Changes of synaptic density in the primary visual cortex of the macaque monkey from fetal to adult stage. *J Neurosci*. 1993;13(7):2801-2820.
23. Jespersen SN, Leigland LA, Cornea A, Kroenke CD. Determination of axonal and dendritic orientation distributions within the developing cerebral cortex by diffusion tensor imaging. *IEEE Trans Med Imaging*. 2012;31(1):16-32.
24. Bock AS, Olavarria JF, Leigland LA, Taber EN, Jespersen SN, Kroenke CD. Diffusion tensor imaging detects early cerebral cortex abnormalities in neuronal architecture induced by bilateral neonatal enucleation: An experimental model in the ferret. *Front Syst Neurosci*. 2010;4:149.
25. Dean JM, McClendon E, Hansen K, *et al*. Prenatal cerebral ischemia disrupts MRI-defined cortical microstructure through disturbances in neuronal arborization. *Sci Transl Med*. 2013;5(168):168ra7.
26. Kroenke CD. Using diffusion anisotropy to study cerebral cortical gray matter development. *J Magn Reson*. 2018;292:106-116.
27. Kroenke CD, Taber EN, Leigland LA, Knutsen AK, Bayly PV. Regional patterns of cerebral cortical differentiation determined by diffusion tensor MRI. *Cereb Cortex*. 2009;19(12):2916-2929.
28. Rathi Y, Pasternak O, Savadjiev P, *et al*. Gray matter alterations in early aging: A diffusion magnetic resonance imaging study. *Hum Brain Mapp*. 2014;35(8):3841-3856.
29. Schlemm E, Schulz R, Bonstrup M, *et al*. Structural brain networks and functional motor outcome after stroke-a prospective cohort study. *Brain Commun*. 2020;2(1):fcaa001.
30. Bonstrup M, Krawinkel L, Schulz R, *et al*. Low-frequency brain oscillations track motor recovery in human stroke. *Ann Neurol*. 2019; 86(6):853-865.
31. Guder S, Frey BM, Backhaus W, *et al*. The influence of corticocerebellarstructural connectivity on cortical excitability in chronic-stroke. *Cereb Cortex*. 2020;30(3):1330-1344.
32. Mayka MA, Corcos DM, Leurgans SE, Vaillancourt DE. Three-dimensional locations and boundaries of motor and premotor cortices as defined by functional brain imaging: A meta-analysis. *Neuroimage*. 2006;31(4):1453-1474.
33. Guder S, Frey BM, Backhaus W, *et al*. The influence of corticocerebellar structural connectivity on cortical excitability in chronic stroke. *Cereb Cortex*. 2020;30(3):1330-1344.
34. Peters DM, Fridriksson J, Richardson JD, *et al*. Upper and lower limb motor function correlates with ipsilesional corticospinal tract and red nucleus structural integrity in chronic stroke: A cross-sectional, ROI-based MRI study. *Behav Neurol*. 2021;2021:3010555.
35. Paul T, Cieslak M, Hensel L, *et al*. The role of corticospinal and extrapyramidal pathways in motor impairment after stroke. *Brain Commun*. 2023;5(1):fcac301.
36. Nemati PR, Backhaus W, Feldheim J, *et al*. Brain network topology early after stroke relates to recovery. *Brain Commun*. 2022;4(2):fcac049.
37. Jenkinson M, Beckmann CF, Behrens TE, Woolrich MW, Smith SM. FSL. *Neuroimage*. 2012;62(2):782-790.
38. Tustison NJ, Cook PA, Klein A, *et al*. Large-scale evaluation of ANTs and FreeSurfer cortical thickness measurements. *Neuroimage*. 2014;99:166-179.
39. Tournier JD, Smith R, Raffelt D, *et al*. MRtrix3: A fast, flexible and open software framework for medical image processing and visualisation. *Neuroimage*. 2019;202:116137.
40. Fischl B, van der Kouwe A, Destrieux C, *et al*. Automatically parcellating the human cerebral cortex. *Cereb Cortex*. 2004;14(1):11-22.
41. Schulz R, Frey BM, Koch P, *et al*. Cortico-cerebellar structural connectivity is related to residual motor output in chronic stroke. *Cereb Cortex*. 2017;27(1):635-645.
42. Wahl M, Lauterbach-Soon B, Hattingen E, *et al*. Human motor corpus callosum: Topography, somatotopy, and link between microstructure and function. *J Neurosci*. 2007;27(45):12132-12138.
43. Schulz R, Zimerman M, Timmermann JE, Wessel MJ, Gerloff C, Hummel FC. White matter integrity of motor connections related to training gains in healthy aging. *Neurobiol Aging*. 2014;35(6): 1404-1411.
44. Meyer BU, Röricht S, Woiciechowsky C. Topography of fibers in the human corpus callosum mediating interhemispheric inhibition between the motor cortices. *Ann Neurol*. 1998;43(3):360-369.
45. Hofer S, Frahm J. Topography of the human corpus callosum revisited–comprehensive fiber tractography using diffusion tensor magnetic resonance imaging. *Neuroimage*. 2006;32(3):989-994.
46. Benjamini Y. Controlling the false discovery rate: A practical and powerful approach to multiple testing. *J R Stat Soc: Ser B (Methodol)*. 1995;57:289-300.
47. Kato J, Yamada T, Kawaguchi H, Matsuda K, Higo N. Functional near-infrared-spectroscopy-based measurement of changes in cortical activity in macaques during post-infarct recovery of manual dexterity. *Sci Rep*. 2020;10(1):6458.
48. Orczykowski ME, Arndt KR, Palitz LE, *et al*. Cell based therapy enhances activation of ventral premotor cortex to improve recovery following primary motor cortex injury. *Exp Neurol*. 2018;305:13-25.
49. Frost SB. Reorganization of remote cortical regions after ischemic brain injury: A potential substrate for stroke recovery. *J Neurophysiol*. 2003;89(6):3205-3214.
50. Dancause N, Barbay S, Frost SB, *et al*. Effects of small ischemic lesions in the primary motor cortex on neurophysiological organization in ventral premotor cortex. *J Neurophysiol*. 2006;96(6): 3506-3511.
51. Rehme AK, Eickhoff SB, Rottschy C, Fink GR, Grefkes C. Activation likelihood estimation meta-analysis of motor-related neural activity after stroke. *Neuroimage*. 2012;59(3): 2771-2782.
52. Rehme AK, Fink GR, Von Cramon DY, Grefkes C. The role of the contralesional motor cortex for motor recovery in the early days after stroke assessed with longitudinal fMRI. *Cereb Cortex*. 2011; 21(4):756-768.
53. Schaechter JD, Perdue KL. Enhanced cortical activation in the contralesional hemisphere of chronic stroke patients in response to motor skill challenge. *Cereb Cortex*. 2008;18(3):638-647.
54. Marconi B, Genovesio A, Giannetti S, Molinari M, Caminiti R. Callosal connections of dorso-lateral premotor cortex. *Eur J Neurosci*. 2003;18(4):775-788.
55. Fiori F, Chiappini E, Avenanti A. Enhanced action performance following TMS manipulation of associative plasticity in ventral premotor-motor pathway. *Neuroimage*. 2018;183:847-858.
56. Boussaoud D, Tanne-Gariepy J, Wannier T, Rouiller EM. Callosal connections of dorsal versus ventral premotor areas in the macaque monkey: A multiple retrograde tracing study. *BMC Neurosci*. 2005; 6:67.
57. Bestmann S, Swayne O, Blankenburg F, *et al*. The role of contralesional dorsal premotor cortex after stroke as studied with concurrent TMS-fMRI. *J Neurosci*. 2010;30(36):11926-11937.
58. Lotze M, Markert J, Sauseng P, Hoppe J, Plewnia C, Gerloff C. The role of multiple contralesional motor areas for complex hand movements after internal capsular lesion. *J Neurosci*. 2006;26(22):6096-6102.
59. Spocter MA, Hopkins WD, Barks SK, *et al*. Neuropil distribution in the cerebral cortex differs between humans and chimpanzees. *J Comp Neurol*. 2012;520(13):2917-2929.